Decolorization of Malachite green dye from wastewater by *Populus deltoides*: three-level Box–Behnken design optimization, equilibrium, and kinetic studies

Afsaneh Shahbazi and Farnoosh Bagheri Zonoz

ABSTRACT

Decolorization of Malachite green in aqueous solution by adsorption onto *Populus deltoides* sawdust (PSD) was optimized through a four-factor, three-level Box–Behnken design in response surface methodology. The influences of four independent variables such as initial pH of solution (3–7), dye concentration (50–300 mg/L), adsorbent dose (0.2–2 g/L), and temperature (23–50 °C) were studied to optimize the condition of dye removal. A natural log transformation was suggested by the Box–Cox plot in order to enhance the model significance. Regression analysis showed good fit of the experimental data to the second-order polynomial model with high coefficient of determination values ($R^2 = 0.996$; $R^2_{adj.} = 0.9913$; $R^2_{pred.} = 0.9769$), *F*-value of 213.03, and *p*-value of <0.0001 ($\alpha = 0.05$). Under optimum values of all the four variables, viz., pH of 6.02, initial dye concentration of 262.6 mg/L, adsorbent dose of 0.23 g/L and temperature of 30.3 °C, the maximum uptake (q_e) was noted to be 920.9 mg/g. The experimental equilibrium adsorption data were fitted well to the Langmuir isotherm model ($R^2 = 0.9949$). Kinetic studies revealed that adsorption followed pseudo-second order. It was found that PSD is suitable for reuse four times in successive adsorption-desorption cycles with loss of 25.2% in adsorption capacity.

Key words | adsorption, desirability function, Malachite green, optimization, poplar sawdust, recovery

Afsaneh Shahbazi (corresponding author)
Farnoosh Bagheri Zonoz
Environmental Sciences Research Institute,
Shahid Beheshti University, G.C.,
Tehran 1983969411,
Iran
E-mail: *a_shahbazi@sbu.ac.ir*

INTRODUCTION

Synthetic dyestuffs have been extensively utilized in many industries including textiles, papers, cottons, wool, leather, and cosmetic products (Roosta *et al.* 2014). Over 7×10^5 tonnes of 10,000 different commercial dyes and pigments are produced annually worldwide with approximately 17,000 tonnes entering industrial wastewaters (Chowdhury *et al.* 2011). The discharge of dye containing effluents into natural water bodies not only can pose hazardous effects on living systems because of the carcinogenic, mutagenic, allergenic, and toxic nature of dyes, but also cause impeding light penetration and inhibiting the growth of biota (Mittal *et al.* 2014). The complex aromatic structure of synthetic dyes is resistant to light, biological activity, ozone, and other degradative environmental conditions. Hence, the treatment of dye contaminated effluents with cost-effective and efficient methods is of high scientific and public interest (Wang *et al.* 2014).

Among the various dyes, triphenylmethane dyes make up an important category in many industrial processes. Malachite green (MG) is a cationic triphenylmethane dye (Figure 1) and most commonly used for the dyeing of cotton, silk, paper, leather, and also in manufacturing of paints and printing inks (Ding *et al.* 2012; Akar *et al.* 2013; Du *et al.* 2013). MG has been listed as a priority chemical for carcinogenicity assessment by the U.S. Food and Drug Administration (Srivastava *et al.* 2004; Shedbalkar & Jadhav 2011). Nonetheless, MG is still utilized in many regions worldwide due to its low cost, good efficacy, and a lack of

doi: 10.2166/wrd.2015.085

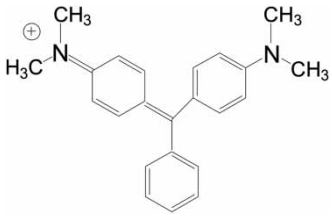

Figure 1 | The chemical structure of MG dye.

suitable alternatives. Therefore, it is of urgency to explore effective methods to solve this problem (Du *et al.* 2013).

Among various conventional methods for removing dyes from wastewater (reverse osmosis, electrodialysis, ultrafiltration, ion-exchange, etc.), removal of dyes by physical adsorption technologies is regarded as one of the competitive methods because of simplicity and flexibility in design, ease of operation, low initial cost, insensitivity to toxic substances, and complete removal of pollutants even from dilute solutions (Chowdhury *et al.* 2011; Wang *et al.* 2014). A large variety of wastes/by-products of industries, such as sawdust, have been employed as inexpensive, eco-friendly, and locally available adsorbents for dye removal from wastewater (Hameed & El-Khaiary 2008). Sawdust contains rich fiber and some functional groups such as amine, carboxyl, hydroxyl, etc., that might be useful for binding dyes (Wan Ngah & Hanafiah 2008). Beech sawdust has been shown to have a maximum adsorption capacity of 83.21 mg/g at 20 °C for removal of MG (Witek-Krowiak 2011). MG biosorption onto rattan sawdust was studied and the maximum adsorption quantity of 62.71 mg/g obtained (Hameed & El-Khaiary 2008). Wang *et al.* (2014) studied MG biosorption onto *Cinnamomum camphora* sawdust modified by various organic acids (oxalic acid, citric acid, and tartaric acid) and obtained a maximum adsorption capacity of 280.3, 222.8, and 157.5 mg/g, respectively.

In Iran, *Populus deltoides* is one of the largest hardwood and fastest growing trees which is widely used in woodcrafts and carpentry. In the present study, the effects of four important process parameters, including pH, adsorbent dosage, initial MG dye concentration, and temperature on MG sorption by poplar (*P. deltoides*) sawdust (PSD) as a low-cost, locally available, and eco-friendly adsorbent were studied using three-level Box–Behnken design (BBD) which provided a mathematical model showing the influence of each variable and their interactions. The aim of this work was also to study the sorption kinetics and equilibrium employing different models.

MATERIALS AND METHODS

Materials and chemicals

MG oxalate, a basic green dye (MG; $C_{52}H_{54}N_4O_{12}$, MW = 927.00 g/mole) was purchase from Merck. The PSD was collected from a local sawmill. It was washed several times with distilled water to remove dust-like and soluble impurities. It was then oven dried at 70 °C for 24 h to constant weight. The dried sample was crushed, sieved to obtain a particle size of 0.5 mm, and stored in glass bottles for later use.

Batch adsorption procedure

Batch experiments were conducted in continuously stirred (150 rpm) conical flasks containing 50 mL of different concentrations of dye solution (50–300 mg/L) and specified amounts of adsorbent (0.2–2 g) in a water bath (23–50 °C) for 24 h. The experiment was conducted at different pH values ranging from 3 to 7. Alkaline pH (above 7) leads to the conversion of MG to Leucomalachite green (Badiei *et al.* 2014). The samples were finally centrifuged and the concentrations of the residual dye concentration in solution was analyzed by a double beam vis-spectrophotometer (HACH Lange DR 2800) at $\lambda_{max} = 619$ nm. The percentage of dye decolorization ($R\%$) and quantity of MG adsorbed onto adsorbent at the time of equilibrium (q_e) were calculated using Equations (1) and (2), respectively (Jain *et al.* 2011; Bingöl *et al.* 2012).

$$R\% = \frac{C_0 - C_e}{C_0} \times 100 \quad (1)$$

$$q_e = \frac{(C_0 - C_e)V}{W} \quad (2)$$

where C_0 and C_e (mg/L) are the liquid-phase concentrations of dye at initial and equilibrium, respectively. V (L) is the

volume of the solution and W (g) is the mass of dry adsorbent used. The pH was adjusted by adding a few drops of diluted 0.1 N, NaOH or 0.1 N, HCl and was measured by using a pH meter. Each experiment was repeated at least three times to observe the reproducibility.

Box–Behnken experimental design and optimization by response surface methodology

Response surface methodology (RSM) is an efficient statistical method that uses quantitative data of appropriate experiments for designing experiments, analyzing the relationships between the dependent variables (responses) and the independent variables (factors) (Das *et al*. 2014), developing response surface models, and ultimately optimizing the process variables to achieve maximum response (Mourabet *et al*. 2012; Akar *et al*. 2014). In this case, the BBD which consists of four factors, each at three levels (three levels, four factorial) was applied to evaluate optimum process conditions and the individual and combined effects of the independent test variables on the response (adsorption capacity).

A second-degree polynomial equation approximated for evaluating the effect of each independent variable on the response is as follows (Akar *et al*. 2014):

$$Y = \beta_0 + \sum_{i=1}^{k} \beta_i x_i + \sum_{i=1}^{k} \beta_{ii} x_i^2 + \sum_{i=1}^{k} \sum_{j=1}^{k} \beta_{ij} x_i x_j + \varepsilon \quad (3)$$

where Y is the process response or output (dependent variable), k is the number of the patterns, i and j are the index numbers for pattern, β_0 is the free or offset term called intercept term, $x_1, x_2, \ldots, x_k$ are the coded independent variables, β_i is the first-order (linear) main effect, β_{ii} is the quadratic (squared) effect, β_{ij} is the interaction effect, and ε is the random error or allows for discrepancies or uncertainties between predicted and measured values. In developing Equation (3), the natural (uncoded) independent variables ($X_1, X_2, \ldots, X_k$) are coded according to the following transformation (Michaux *et al*. 2013):

$$x_i = \frac{X_i - X_0}{\Delta X_i}, \quad i = 1, 2, 3, \ldots, k \quad (4)$$

where x_i is the dimensionless coded value of the ith independent variable, X_i is the uncoded value of the ith independent variable, X_0 is the uncoded ith independent variable at the center point, and ΔX_i is the step change value.

For this study, the effects of initial pH of solution (pH: 3–7), initial dye concentration (C_0: 50–300 mg/L), adsorbent dose (D: 0.2–2 g/L), and temperature (T: 23–50 °C), that predominantly affected the extent of adsorption by PSD were identified as the independent test variables design of the experiment (as X_1, X_2, X_3, and X_4, respectively). The low, middle, and high levels of each variable were designated as −1, 0, and +1, respectively. The experimental range and levels of independent variables are presented in Table 1. The central values chosen for the experimental design were pH = 5, C_0 = 175 mg/L, D = 1.1 g/L, and T = 36.5 °C in uncoded form. The number of experiments (N) required for the development of BBD is defined as $N = 2k(k-1) +$ CP (where k is number of factors and CP is the number of central points). As seen in Table 2, a total of 27 experiments were developed by BBD for adsorption of MG.

A multiple regression modeling and graphical analyses of the experimental data were obtained using Design-Expert software version 8.0 (Stat-Ease, Minneapolis, MN, USA). The significance of independent variables and their interactions were tested by means of the analysis of variance (ANOVA). An alpha (α) level of 0.05 and p-value <0.05 were used to determine the statistical significance in all analyses. The results were assessed with various descriptive statistics such as t-ratio, p-value, F-value, degrees of freedom (df),

Table 1 | Experimental range and levels of independent variables

	Range and levels			
Variables	**Low level (−1)**	**Center level (0)**	**High level (+1)**	**ΔX_i[a]**
Initial pH of solution (pH), X_1	3 (−1)	5 (0)	7 (1)	2
Initial dye concentration (C_0), X_2	50 (−1)	175 (0)	300 (1)	125
Adsorbent dosage (d), X_3	0.2 (−1)	1.1 (0)	2 (1)	0.9
Temperature (T), X_4	23 (−1)	36.5 (0)	50 (1)	13.5

[a]Step change values.

Table 2 | BBD matrix with four independent variables (expressed coded) and two response ($q_e \pm SD$ and $R\% \pm SD$)

Run no.	Initial pH of solution (pH) x_1 (coded)	Initial dye concentration (C_0: mg/L) x_2 (coded)	Adsorbent dosage (d: g/L) x_3 (coded)	Temperature (T: °C) x_4 (coded)	Adsorption efficiency	
					R%	q_e (mg/g)
1	−1	−1	0	0	76.48 ± 0.02	34.8 ± 0.02
2	+1	−1	0	0	98.62 ± 0.01	44.8 ± 0.01
3	−1	1	0	0	46.02 ± 0.01	126.0 ± 0.01
4	+1	1	0	0	82.72 ± 0.05	226.0 ± 0.05
5	0	0	−1	−1	53.98 ± 0.02	472.3 ± 0.02
6	0	0	1	−1	88.57 ± 0.02	70.2 ± 0.02
7	0	0	−1	1	70.38 ± 0.06	616.0 ± 0.06
8	0	0	1	1	80.25 ± 0.02	77.5 ± 0.02
9	−1	0	0	−1	37.82 ± 0.01	60.2 ± 0.01
10	1	0	0	−1	76.45 ± 0.02	122.0 ± 0.02
11	−1	0	0	1	63.79 ± 0.03	101.0 ± 0.03
12	1	0	0	1	80.43 ± 0.03	128.0 ± 0.03
13	0	−1	−1	0	72.32 ± 0.01	181.0 ± 0.01
14	0	1	−1	0	59.46 ± 0.02	892.0 ± 0.02
15	0	−1	1	0	97.76 ± 0.02	24.4 ± 0.02
16	0	1	1	0	82.93 ± 0.01	124.0 ± 0.01
17	−1	0	−1	0	41.12 ± 0.02	360.0 ± 0.02
18	1	0	−1	0	98.52 ± 0.06	862.0 ± 0.06
19	−1	0	1	0	59.77 ± 0.03	60.0 ± 0.03
20	1	0	1	0	92.64 ± 0.02	81.1 ± 0.02
21	0	−1	0	−1	95.48 ± 0.03	42.0 ± 0.03
22	0	1	0	−1	83.25 ± 0.04	170.0 ± 0.04
23	0	−1	0	1	93.04 ± 0.01	46.0 ± 0.01
24	0	1	0	1	61.39 ± 0.03	240.0 ± 0.03
25	0	0	0	0	73.30 ± 0.05	115.0 ± 0.05
26	0	0	0	0	72.20 ± 0.04	115.0 ± 0.04
27	0	0	0	0	73.30 ± 0.01	34.8 ± 0.01

coefficient of variation (CV), determination coefficient (R^2), adjusted determination coefficient ($R^2_{adj.}$), correlation coefficient (R), sum of squares (SS), and mean sum of squares (MSS) statistic to reflect the statistical significance of the quadratic model. The analysis was focused on verifying the influence of individual parameters on adsorption capacity of PSD for MG removal.

The desirability function was used to evaluate all the factors and response in the adsorption experiments in order to find an optimum point where the desired conditions could be obtained.

Equilibrium and kinetic studies

Adsorption isotherms were performed in a set of Erlenmeyer flasks (250 mL) containing solutions of dye (200 mL) with different initial concentrations (50–300 mg/L). Equal mass of 0.046 g of PSD was added to dye solutions and kept in an isothermal shaker (30 ± 0.5 °C) for 3 h to reach equilibrium of the solid–solution mixture. The equilibrium data were analyzed using various isotherm models of Langmuir, Freundlich, Redlich–Peterson, and Fritz–Schlunder. The effect of contact time between solution and adsorbent was

investigated to analyze the adsorption kinetics at the optimized conditions of pH, C_0, D, and T. The samples were taken at various times selected from 5 min to 3 h and the concentrations of the residual dye in solution were analyzed by a double beam vis-spectrophotometer (HACH Lange DR 2800) at $\lambda_{max=}$619 nm.

RESULTS AND DISCUSSION

Optimization of adsorption conditions using RSM approach

Statistical approaches with a BBD were used for efficient adsorption of MG and for determining the interaction between effective factors including pH, adsorbent dose (g/L), initial dye concentration (mg/L), and temperature (°C). Among 27 designed experiments, a maximum adsorption capacity of 892 mg/g was noted at the factors pH 5, PSD dosage 0.2 g/L, initial MG concentration 300 mg/L, and temperature 36.5 °C (Table 2).

In the present study, Box–Cox plot was used to check the value of lambda (λ) which was generally used to predict any necessary transformation of the experimental value in order to enhance the model significance. A natural log transformation (ln) was used based on the lambda value of 0 as obtained from the plot (Figure 2). The plot showed the minimum lambda values, as well as lambdas at the 95% confidence range.

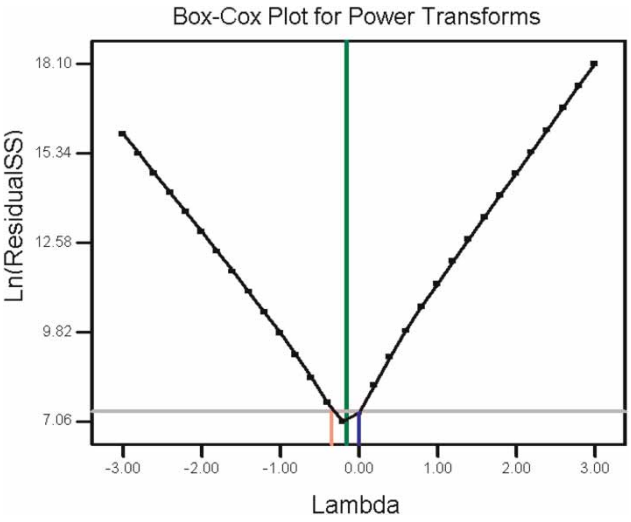

Figure 2 | Box–Cox plot and the value of lambda (λ).

By applying multiple regression analysis on the design matrix and the responses (q_e), the following second-order polynomial equation in terms of coded factors was established to explain the removal efficiency:

$$Y = 4.74 + 0.26x_1 + 0.76x_2 - 1.01x_3 + 0.11x_4 + 0.083x_1x_2 - 0.14x_1x_3 - 0.12x_1x_4 + 0.0076x_2x_3 - 0.063x_2x_4 - 0.032x_3x_4 - 0.088x_1^2 - 0.26x_2^2 + 0.57x_3^2 - 0.0061x_4^2 \quad (5)$$

where Y is the $\ln(q_e)$, x_1, x_2, x_3, and x_4 are the coded terms for four independent test variables, pH, C_0, D, and T, respectively.

ANOVA for ln (natural log) transformed response surface quadratic model was conducted to test the significance of the fit of the second-order polynomial equation for the experimental data as given in Table 3.

The results of ANOVA for response surface quadratic model for the prediction of MG removal efficiency (Table 3) confirmed that the quadratic model was highly significant according to F_{model}-value of 213.03 and a very low-probability value of <0.0001. The high value of determination coefficient ($R^2 = 0.9960$) indicated goodness-of-fit of the model. In addition, the value of adjusted determination coefficient ($R^2_{\text{adj.}} = 0.9913$) was also very high, showing a high significance of the model. Furthermore, a very high value of the predicted determination coefficient ($R^2_{\text{pred.}} = 0.9769$) confirmed an excellent correlation between the predicted values (responses) and the experimental results. The adequate precision which measures the signal to noise ratio was obtained greater than 4 (adeq precision = 53.76) indicating an adequate signal. Very high degree of precision (53.76) and a low value of the coefficient of variation (CV = 1.18%) confirmed the precision and reliability of the experiments carried out and that the model can be used to navigate the design space.

To assess calibration of probability predictions and check for bias, predicted, and observed responses were compared (Table 4). The low value of residuals (difference between predicted and observed responses) showed the accuracy of the predictive model. The normal % probability and studentized

Table 3 | ANOVA for response surface quadratic model for the prediction of MG removal efficiency

	Statistics					
Factors (coded)	**Sum of squares (SS)**	**Degrees of freedom (df)**	**Mean squares (MSS)**	***F*-value**	**Probability (p) > F ***	**PC%**
Model	23.46	14	1.68	213.03	< 0.0001	–
x_1	0.73	1	0.73	92.47	< 0.0001	3.234
x_2	7.02	1	7.02	891.90	< 0.0001	31.225
x_3	12.30	1	12.30	1,563.40	< 0.0001	54.711
x_4	0.15	1	0.15	18.71	0.0010	0.007
$x_{1\times 2}$	0.03	1	0.03	3.50	0.0861	0.122
$x_{1\times 3}$	0.08	1	0.08	10.39	0.0073	0.363
$x_{1\times 4}$	0.06	1	0.06	7.00	0.0213	0.245
$x_{2\times 3}$	0.00	1	0.00	0.03	0.8654	0.001
$x_{2\times 4}$	0.02	1	0.02	2.05	0.1779	0.072
$x_{3\times 4}$	0.00	1	0.00	0.54	0.4780	0.019
x_1^2	0.04	1	0.04	5.30	0.0400	0.185
x_2^2	0.34	1	0.34	43.31	< 0.0001	1.517
x_3^2	1.72	1	1.72	218.46	< 0.0001	7.651
x_4^2	0.00	1	0.00	0.03	0.8749	0.001
Residual	0.09	12	0.01			
Lack of fit	0.09	10	0.01			
Pure error	0.00	2	0.00			
Cor total	23.56	26				

*p-values <0.05 were considered to be significant.

residuals plots are shown in Figure 3. A straight line formed from the points confirmed that the error terms are, indeed, normally distributed, and independent of each other.

The desirability function was used to simultaneously optimize adsorption condition to obtain maximum response. Hence, the numerical optimization was developed by choosing the desired goal for each factor and response. The scale of the desirability function ranged between $d = 0$ (for an unacceptable response value) and $d = 1$ (for a completely desirable one). Desirability condition of the numerical optimization of four independent variables, namely initial solution pH, initial dye concentration, adsorbent dose, and response of adsorption capacity is shown in Figure 4. For optimization results, a maximum adsorption capacity of 920.9 mg/g was achieved with favorable desirability of 1.00 at optimum adsorption condition of initial pH of solution (6.02), initial concentration (262.6 mg/L), adsorbent dosage (0.23 g/L), and temperature (30.3 °C).

An additional experiment was then performed at suggested optimum adsorption condition to confirm the optimum results and their validation. The results were closely related with the data obtained from optimization analysis using desirability functions, indicating BBD incorporated with desirability functions could be effectively used to optimize the adsorption parameters for the removal of MG by PSD.

Interactive effect of model components on MG removal

To investigate the integrated effect of initial dye concentration, initial solution pH, amount of adsorbent, and temperature, the RSM was used and the result shown in the form of three-dimensional (3D) plots. The interactions between initial pH of solution (X_1) and initial concentration of MG (X_2) is shown in Figure 5(a). From the results (Figure 5(a)), an excess of MG molecules in the solution in

Table 4 | Observed responses and predicted values with residuals

Batch no.	Coded factors				Natural log of MG sorption efficiency (mg/g)[a]		Rounded residuals ($Y_o - Y_p$)	Error (%)
	x_1	x_2	x_3	x_4	Observed, Y_o	Predicted, Y_p		
1	−1	−1	0	0	3.55	3.48	0.074	2.08
2	+1	−1	0	0	3.80	3.80	0.000	0.00
3	−1	1	0	0	4.84	4.84	−0.003	−0.06
4	+1	1	0	0	5.42	5.50	−0.077	−1.42
5	0	0	−1	−1	6.19	6.18	0.019	0.30
6	0	0	1	−1	4.25	4.22	0.036	0.84
7	0	0	−1	1	6.42	6.46	−0.039	−0.60
8	0	0	1	1	4.35	4.37	−0.022	−0.51
9	−1	0	0	−1	4.10	4.18	−0.078	−1.91
10	1	0	0	−1	4.80	4.90	−0.099	−2.06
11	−1	0	0	1	4.62	4.63	−0.017	−0.37
12	1	0	0	1	4.85	4.89	−0.038	−0.78
13	0	−1	−1	0	5.20	5.32	−0.117	−2.25
14	0	1	−1	0	6.79	6.83	−0.036	−0.53
15	0	−1	1	0	3.19	3.28	−0.081	−2.52
16	0	1	1	0	4.82	4.82	0.001	0.01
17	−1	0	−1	0	5.89	5.85	0.039	0.66
18	1	0	−1	0	6.76	6.63	0.134	1.98
19	−1	0	1	0	4.09	4.11	−0.014	−0.35
20	1	0	1	0	4.40	4.32	0.081	1.83
21	0	−1	0	−1	3.74	3.67	0.064	1.70
22	0	1	0	−1	5.14	5.08	0.059	1.16
23	0	−1	0	1	3.83	3.77	0.060	1.57
24	0	1	0	1	5.48	5.42	0.056	1.02
25	0	0	0	0	4.74	4.74	0.000	0.00
26	0	0	0	0	4.74	4.74	0.000	0.00
27	0	0	0	0	4.74	4.74	0.000	0.00

[a]Y is $\ln(q_e)$.

the presence of a high level of pH could promote sorption capacity. As a rule, increasing the initial dye concentration provides a driving force to overcome all mass transfer resistances of dyes between the aqueous and solid phase resulting in an increase in the adsorption capacity. However as shown in Table 2, the removal percentage (R%) decreased from 98.6 to about 82.7% with increasing dye concentration from 50 to 300 mg/L, while the PSD dosage and temperature were set at 1.1 g/L and 36.5 °C, respectively. It could be explained by the fact that the adsorbent has a limited number of active sites, which become saturated at a certain concentration. From this 3D plot, a maximal adsorption capacity of 245 mg/g was achieved at an initial solution pH of 7.0 and dye concentration of 300 mg/L, while the PSD dosage and temperature were set at the middle value. It is evident from Figure 5(b) that both the independent variables of initial solution pH and PSD dosage had a strong influence on the dye sorption capacity. From this plot, the adsorption capacity (q_e) decreases with an increase in PSD dosage. Figure 5(c) shows the interaction between pH and

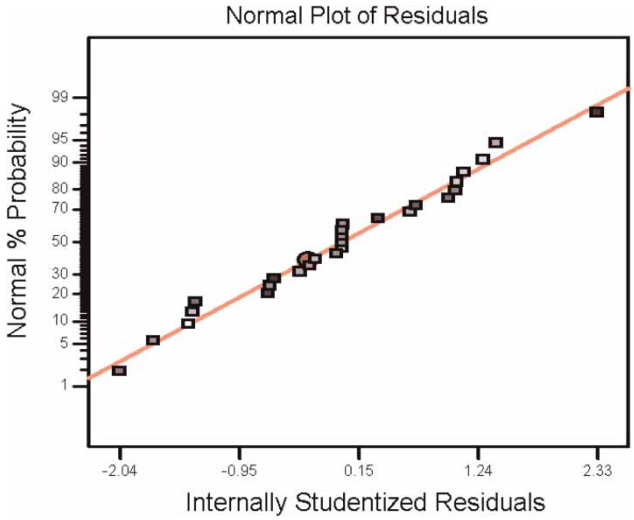

Figure 3 | The studentized residuals and normal % probability plot of the multiple regression model.

realizing the percentage of contributions (PC) of each model parameter onto MG adsorption the PC was calculated from the sum of squares for each individual model component in ANOVA. The total percentage of contribution (TPC) values for the possible first-order (TPC_i), quadratic (TPC_{ii}), and interaction terms (TPC_{ij}) are calculated by Equations (6)–(8) and the results shown in Figure 6.

$$TPC_i = \frac{\sum_{i=1}^{n} SS_i}{\sum_{i=1}^{n}\sum_{i=1}^{n} SS_i + SS_{ii} + SS_{ij}} \times 100 \quad (6)$$

$$TPC_{ii} = \frac{\sum_{i=1}^{n} SS_{ii}}{\sum_{i=1}^{n}\sum_{j=1}^{n} SS_i + SS_{ii} + SS_{ij}} \times 100 \quad (7)$$

$$TPC_{ij} = \frac{\sum_{i=1}^{n}\sum_{i=1}^{n} SS_{ij}}{\sum_{i=1}^{n}\sum_{j=1}^{n} SS_i + SS_{ii} + SS_{ij}} \times 100 \quad (8)$$

temperature. It was observed that the adsorption increases with increasing temperature and pH. The combined effect of initial MG concentration and the PSD dosage on q_e are given in Figure 5(d). As indicated (Figure 5(d)), with an increase in the dye concentration, the removal efficiency (q_e) increased with decreasing PSD dosage until it reached the optimum grade.

However, the results (Table 3) showed that the first-order main effects of the four studied factors were more significant than their respective quadratic effects, but for

As seen in Figure 6, the PSD dosage (x_3) showed the highest level of significance with a contribution of 54.91% as compared to other components. Thus, the adsorption capacity was found to be strongly dependent on adsorbent dosage. In addition, the TPC of first-order terms (TPC_i) demonstrated the highest level of significance with a total contribution of 89.78% as compared to other TPC values. This was followed by the quadratic terms (TPC_{ii}) and interaction terms (TPC_{ij}) with a total contribution of 9.35 and 0.82%, respectively. Therefore, the interaction components

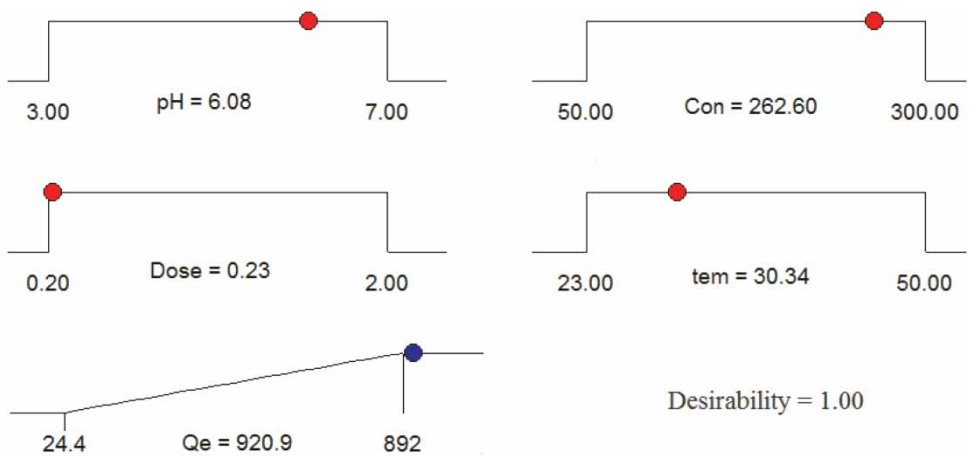

Figure 4 | Desirability of numerical optimization of four independent variables, namely initial solution pH, initial dye concentration, adsorbent dose, and adsorption capacity of MG onto PSD.

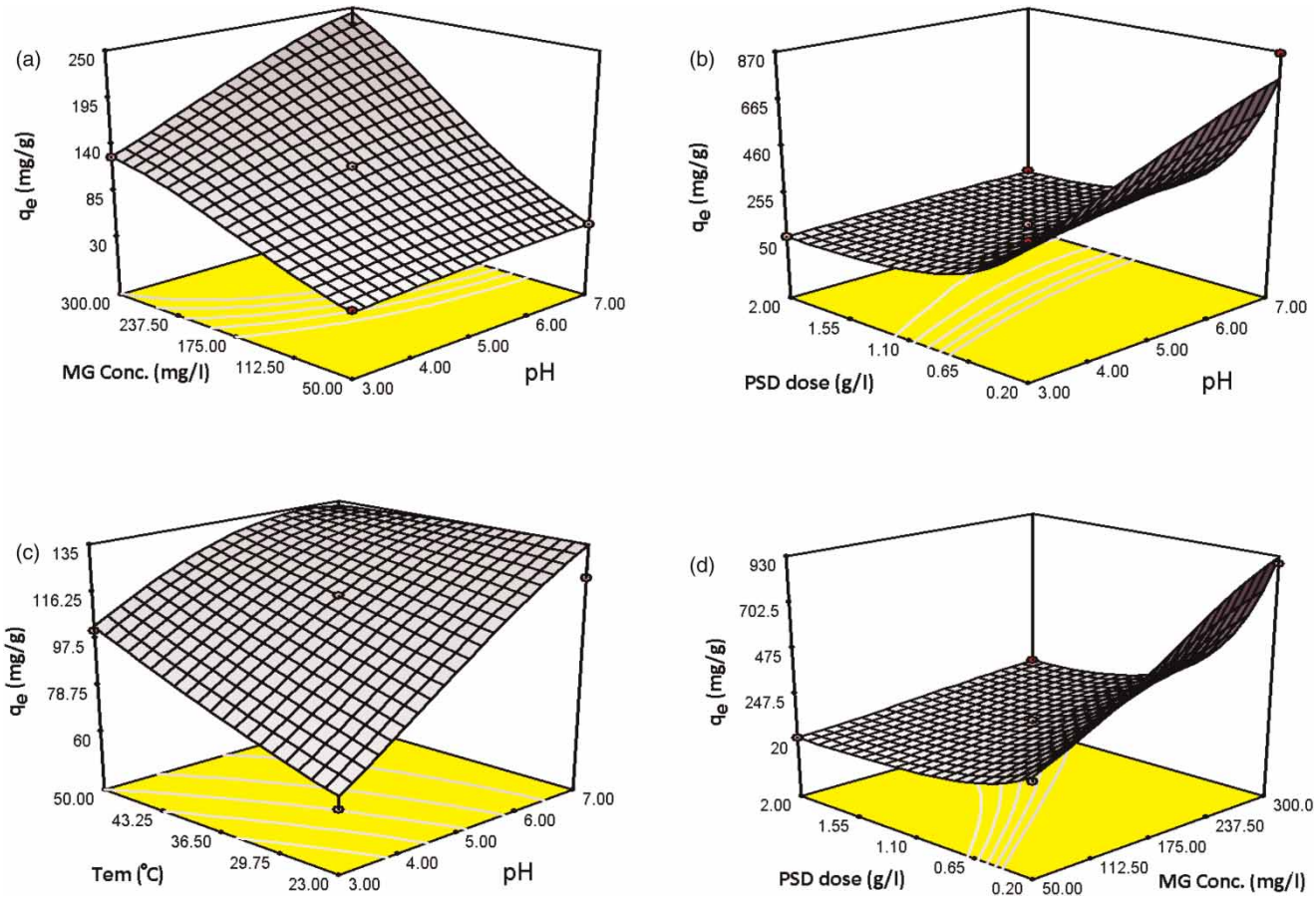

Figure 5 | Three-dimensional response surface diagrams showing the effects of the interactions between two independent variables (other variables were held at their respective center levels): (a) initial pH of solution (X_1) and initial concentration of MG (X_2); (b) initial pH of solution (X_1) and PSD dosage (X_3); (c) initial pH of solution (X_1) and temperature (X_4); (d) initial concentration of MG (X_2), and PSD dosage (X_3).

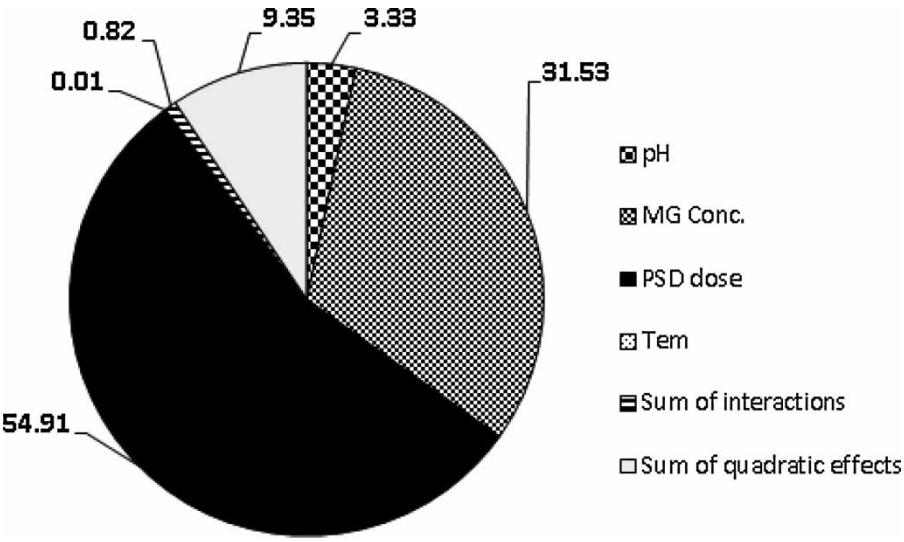

Figure 6 | The percentage contributions (PC%) of model components.

had no effective influence on prediction of the MG adsorption efficiency.

Equilibrium and kinetic studies

To examine the relationship between sorbate and sorbent at equilibrium, the Langmuir (Equation (9)), Freundlich (Equation (10)), Redlich–Peterson (Equation (11)), and Fritz–Schlunder (Equation (12)) isotherm models (Kumar *et al.* 2003) were employed for fitting the equilibrium data and the results are shown in Figure 7.

$$q_e = \frac{q_{max} b C_e}{1 + b C_e} \tag{9}$$

$$q_e = K_f C_e^{1/n} \tag{10}$$

$$q_e = \frac{q_{max} b C_e}{1 + b C_e} \tag{11}$$

$$q_e = \frac{\alpha_1 C_e^{\beta_1}}{1 + \alpha_2 C_e^{\beta_2}} \tag{12}$$

where q_e and q_{max} are the equilibrium and maximum MG loaded by the PSD (mg/g), respectively, C_e is the equilibrium MG concentration in the solution (mg/L). b is the constant that refers to the bonding energy of adsorption (1/g). K_f is the constant related to the adsorption capacity of the adsorbent, and n is the empirical constant related to the intensity of adsorption. K_1 in l/g, K_2 in $(1/mg)^m$, and m are the constants in the Redlich–Peterson isotherm model. α_1 in $(mg/g)/(mg/L)^{\beta 1}$, α_2 in $(mg/g)/(mg/L)^{\beta 2}$, β_1, and β_2 are the constants in the Fritz–Schlunder isotherm model.

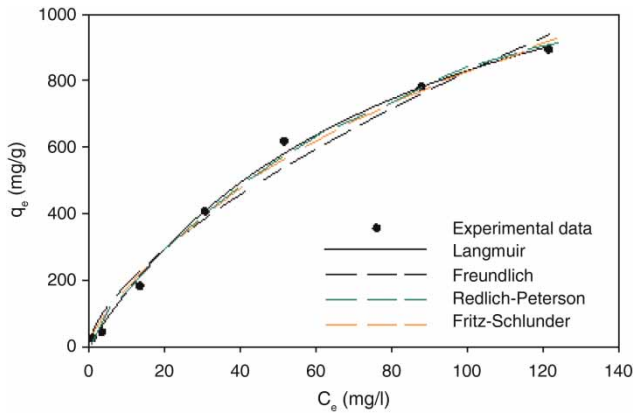

Figure 7 | Isotherm modeling of adsorption of MG onto PSD.

The values of all constants and the non-linear regression correlation coefficients (R^2) for studied isotherm models are summarized in Table 5. Based on the standard error function and R^2 values (Table 5), the applicability of the isotherms was compared. Between the two studied isotherms, it could be concluded that the adsorption of MG onto PSD best fitted to the Langmuir due to a high correlation coefficient value of 0.995 thereby suggesting that adsorption of MG onto PSD was monolayer applicable to homogeneous surfaces. A steep initial slope of the sorption isotherm indicated a high affinity of the adsorbent for the sorbate. The decrease in the slope value could be attributed to the unavailability of vacant sites.

Table 5 | Langmuir, Freundlich, Redlich–Peterson, and Fritz–Schlunder isotherm parameters for adsorption of MG onto PSD

Isotherm model	Parameter	Value
Langmuir	q_m (mg/g)	1,532
	b (l/g)	0.0118
	R^2 (R^2)	0.9949
	Adj R^2 (R_a^2)	0.9932
	Standard error of estimate	31.74
	R_L	0.06
Freundlich	K_f (mg/g)$(mg/L)^{1/n}$	41.87
	N	1.54
	R^2 (R^2)	0.9803
	Adj. R^2 (R_a^2)	0.9764
	Standard error of estimate	54.25
	K_1 (l/g)	0.0139
	K_2 $(l/mg)^m$	1.35
Redlich–Peterson	M	0.077
	R^2 (R^2)	0.9890
	Adj. R^2 (R_a^2)	0.9804
	Standard error of estimate	41.01
	α_1 $(mg/g)/(mg/L)^{\beta 1}$	40.46
	α_2 $(mg/g)/(mg/L)^{\beta 2}$	2.59
Fritz–Schlunder	β_1	2.83
	β_2	2.05
	R^2 (R^2)	0.9880
	Adj. R^2 (R_a^2)	0.9770
	Standard error of estimate	49.77

To predict the favorability of adsorption system, R_L, a dimensionless separation factor was calculated by Equation (13):

$$R_L = \frac{1}{1 + bC_0} \tag{13}$$

where b is the Langmuir constant (l/g) and C_0 is the initial metal ions concentration (mg/L). The value of R_L indicates if the type of Langmuir isotherm is irreversible ($R_L = 0$), favorable ($0 < R_L < 1$) or unfavorable ($R_L > 1$). The separation factor (R_L) is summarized in Table 5, i.e., $0 < R_L < 1$. It revealed that the adsorption of MG onto PSD was favorable.

The kinetic of adsorption was studied by collecting samples from the flasks at predetermined time intervals for analyzing the residual dye concentration in the solution. It was seen that the adsorption of MG increased with a rise in contact time up to 90 min. Further increase in contact time did not enhance the adsorption. Among kinetic models which were exploited to test the experimental data, the non-linear forms of pseudo-first-order and pseudo-second-order kinetic models (Equations (14) and (15), respectively) were applied to experimental kinetic data (Figure 8(a)) in order to investigate the behavior of MG adsorption onto PSD.

$$q_t = q_e(1 - \exp^{-k_1 t}) \tag{14}$$

$$\frac{dq}{dt} = k_2(q_e - q_t)^2 \tag{15}$$

where q_e and q_t are the adsorbed MG in mg/g on the PSD at equilibrium and time t, respectively, k_1 is the constant of first-order adsorption in min^{-1} and k_2 is the rate constant of second-order adsorption in g/mg min (Kumar *et al.* 2003; Chowdhury *et al.* 2011).

According to Figure 8(a), the pseudo-second-order kinetic model with high correlation coefficient ($R^2 = 0.998$, $p < 0.0001$) could provide an accurate fit of the experimental data. In addition, there was a small difference between the experimental and calculated (649 mg/g versus 665 mg/g) to strengthen the applicability of the pseudo-second-order model. The k_2 value calculated from the pseudo-second-order kinetic model was 0.0006 mg/g min.

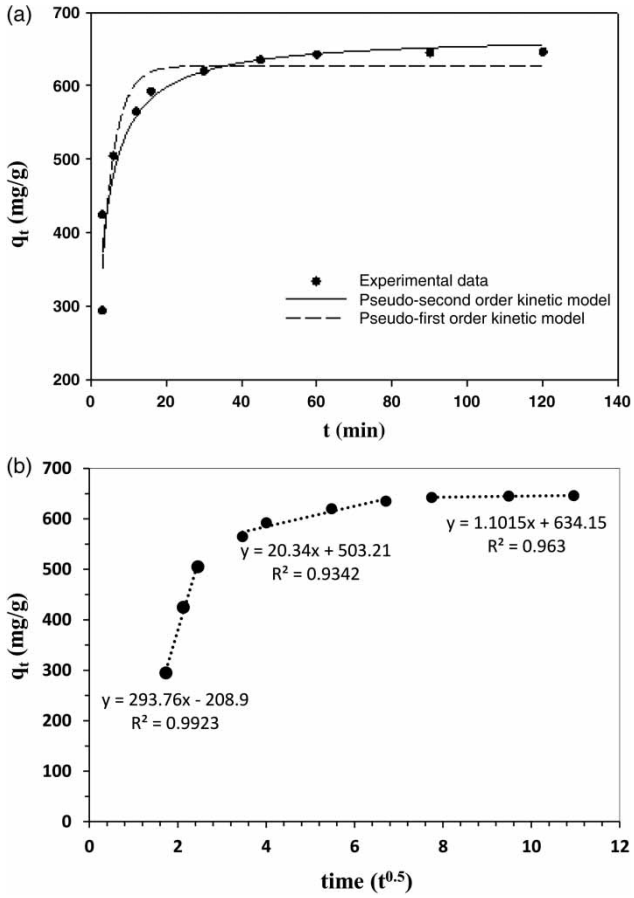

Figure 8 | Kinetic modeling of adsorption of MG onto PSD: (a) pseudo-first-order and pseudo-second-order kinetic models; (b) intraparticle diffusion kinetic model.

Because the pseudo-second-order kinetic models could not identify if film or pore diffusion was the rate-limiting stage in the adsorption, the kinetic data were further analyzed by intraparticle diffusion model, which can be described as (Chowdhury *et al.* 2011; Badiei *et al.* 2014)

$$q_t = k_{id} t^{\frac{1}{2}} + C \tag{16}$$

where k_{id} (mg/g $min^{0.5}$) is the intraparticle diffusion rate constant and C the y-intercept. Intraparticle diffusion was characterized by using the plot of q_t versus square root of time ($t^{1/2}$), described in Figure 8(b). This plot provides clear evidence that the sorption process of MG onto PSD consists of three stages, suggesting that the intraparticle diffusion might not be the only rate-limiting step for the whole reaction (Shahbazi *et al.* 2014). The slope of the linear portion indicates the rate of the sorption. The initial fast rate stage, finished in

5 min, was attributed to the diffusion of ions through the solution to the easily accessible sites on the external surface of the PSD indicating an exterior mass transfer. With the saturation of the external sites, besides the decreasing concentration, intraparticle or pore diffusion took place according to the second linear portion of the plot. This stage was much slower than the initial stage. The third linear portion of the plot corresponds to the sorption at equilibrium.

Application of PSD in real textile effluent

The feasibility and adsorption performance of PSD was also tested using real textile effluent. The characteristics of real wastewater were analyzed before adding PSD. The pH of the effluent was found to be 7.23. Total dissolved solids (TDS), total solids, and chemical oxygen demand (COD) in the effluent were found to be 1,197, 1,094, and 2,416 mg/L, respectively. The concentration of MG was found to be 2,416 mg/L in the real wastewater. The adsorptive removal experiment was conducted at optimum condition (pH of 6.0, PDS dose of 0.23 g/L, and temperature of $30 \pm 0.5\ ^{\circ}C$) in Erlenmeyer flasks (250 mL) containing 200 mL of real wastewater. The mixture was then magnetically stirred at 150 rpm for 3 h to reach equilibrium. For comparison purposes, the removal of dye from synthetic wastewater (dye + distilled water) was also studied at the same conditions as real effluent (dye concentration of 96 mg/L, pH of 6.0, PDS dose of 0.23 g/L, and temperature of $30 \pm 0.5\ ^{\circ}C$). By comparing the percentage removal of dye from synthetic and real wastewater in the same experimental conditions (99.8 versus 80.5%), it is seen that the adsorption efficiency of PSD was not equal for both wastewaters. Hence, sorption capacity may deviate a little from the predicted behavior of PSD based on complexity of real effluents. It was found that after the adsorption process, the concentrations of TDS and COD in untreated effluent were decreased by about 32% (from 1,197 to 813 mg/L) and 45% (from 2,416 to 1,087 mg/L) indicating that some free cationic ions in the real wastewater adsorbed onto PSD, leading to a lesser dye removal.

Recovery experiment

The regenerability of adsorbent is one of the criterion characteristics of sorbent that make the treatment process more economical, particularly for industrial practice. Hence, the regenerability of PSD was evaluated by collecting sorbent after adsorption experiments at optimum condition and recovery by acetone as eluent. The PSD was reused for four successive cycles to determine its reusability. The dye recovery was calculated by the following equation (Shahbazi *et al*. 2014):

$$\text{Dye recovery} = \frac{\text{Amount of dye desorbed}}{\text{Amount of dye adsorbed}} \times 100 \quad (17)$$

The results of recovery experiments are summarized in Table 6. The adsorption capacity of the PSD after two, three, and four cycles indicated a loss in the adsorption capacity of 5.5, 11.8, and 25.2% for MG, indicating an approximately good regeneration capacity of the adsorbent.

Comparison of PSD with other sorbents

A comparison of the PSD capacity for MG removal with that of other similar available agricultural wastes and sawdust is summarized in Table 7. The comparison shows that PSD has a really higher adsorption capacity of MG than many of the other reported adsorbents. A maximum adsorption capacity of 4.354, 20.26, 62.71, 101.31, 117.647, 196.08, 267, and 280.3 mg/g was reported for MG by using neem sawdust, degreased coffee bean, rattan sawdust, NaOH-modified mice musk, *Pithophora* sp., functionalization of sawdust with monosodium glutamate, eggshells and *Cinnamomum camphora* sawdust modified by oxalic acid, respectively, which are approximately 198, 42, 13, 8, 7, 4, 3, and 3 times lower than that obtained by PSD in this study (Kumar *et al*. 2005; Hameed & El-Khaiary 2008; Gong *et al*. 2009; Khattri & Singh 2009; Baek *et al*. 2010;

Table 6 | The four successive adsorption-desorption cycles of MG onto PSD

No. of ads./des. cycles	q_e (mg/g)	Dye recovery%
1	919.3	95
2	868.7	90
3	766.2	86
4	573.1	85

Table 7 | Comparison of MG adsorption capacity of PSD with other reported low-cost adsorbents

	Conditions							
Adsorbents	**Dye Con. (mg/L)**	**Dose (g/L)**	**Temp. (°C)**	**Time (min)**	**pH**	***R*%**	**q_e (mg/g)**	**Reference**
Poplar (*Popolus deltuide*s) sawdust	175	0.2	36.5	90	7	98.52	862.1	This study
Degreased coffee bean	100	6	25 ± 0.1	30	4	98	20.26	Baek *et al.* (2010)
Cinnamomum camphora sawdust modified by oxalic acid	200	1	59.85	720	8	-	280.3	Wang *et al.* (2014)
Pithophora sp.	100	1	30	–	5	–	117.64	Kumar *et al.* (2005)
Eggshells	388	1	–	180	6	–	267.0	Podstawczyk *et al.* (2014)
Neem sawdust	8	2.5	30 ± 1	–	7.2	88.11	4.35	Khattri & Singh (2009)
Rattan sawdust	120	1.5.	30	210	–	–	62.71	Hameed & El-Khaiary (2008)
Functionalization of sawdust with monosodium glutamate	250	2	–	–	6	95	196.08	Gong *et al.* (2009)
NaOH-modified rice husk	500	–	–	132	7	–	101.31	Chowdhury *et al.* (2011)

Chowdhury *et al.* 2011; Podstawczyk *et al.* 2014; Wang *et al.* 2014). The easy availability in abundance, eco-friendly traits, and very low cost of PSD, as well as its high efficiency in MG adsorption reflects a promising utilization in MG removal from aqueous solutions.

CONCLUSION

A four factor, three-level Box–Behnken response surface quadratic model was applied as a mathematical methodology to provide a critical analysis of the simultaneous interactive effects of independent variables, including initial pH of the solution (3–7), initial concentration of MG dye (50–300 mg/L), PSD dosage (0.2–2 g/L), and temperature (23–50 °C), for better understanding of MG removal process. Through 27 runs of designed experiments, maximum adsorption capacity of 892 mg/g was achieved at the factors pH 5, PSD dosage 0.2 g/L, initial MG concentration 300 mg/L, and temperature 36.5 °C. A small difference between the predicted values obtained using the quadratic model and the observed values ($R^2 = 0.9960$; $R^2_{\text{adj.}} = 0.9913$; $R^2_{\text{pred.}} = 0.9769$; adeq precision = 53.76; CV = 1.18%) confirmed adequacy of the developed mathematical model. The statistical results showed that the total effect of first-order terms of the independent variables was significantly justified by a contribution of 89.78% as compared to quadratic terms and interaction terms indicating that the selected variables had a direct relationship on the MG removal efficiency. The PSD dosage was found to be most significant component of the quadratic model (PC = 54.91%). Experimental equilibrium data provided the best fit with the Langmuir isotherm model, indicating monolayer sorption on a homogenous surface. The adsorption kinetics followed the pseudo-second-order kinetic model. However, the sorption process of MG onto PSD consists of three stages, suggesting that the intra-particle diffusion might not be the only rate-limiting step for the whole reaction. The PSD was reused for four successive cycles with a loss in the adsorption capacity of 25.2% after four adsorption-desorption cycles. The absorption capacity of PSD for MG removal was generally higher than the previously reported values. Hence, the PSD waste material seems to be a feasible and affordable option for dye removal because of its eco-friendly traits, availability in abundance, low cost and, in addition, its high sorption capacity.

ACKNOWLEDGEMENT

The authors are grateful to Shahid Beheshti University (SBU) for laboratory support.

REFERENCES

Akar, E., Altinişik, A. & Seki, Y. 2013 Using of activated carbon produced from spent tea leaves for the removal of malachite green from aqueous solution. *Ecol. Eng.* **52**, 19–27.

Akar, S. T., Sayin, F., Turkyilmaz, S. & Akar, T. 2014 Multivariate optimization of the decolorization process by surface modified biomaterial: Box–Behnken design and mechanism analysis. *Environ. Sci. Pollut. Res.* **21**, 13055–13068.

Badiei, A., Mirahsani, A., Shahbazi, A., Younesi, H. & Alizadeh, M. 2014 Adsorptive removal of toxic dye from aqueous solution and real industrial effluent by tris (2-aminoethyl) amine functionalized nanoporous silica. *Environ. Prog. Sustain. Energ.* **33**, 1242–1250.

Baek, M.-H., Ijagbemi, C. O. & Kim, D.-S. 2010 Removal of Malachite Green from aqueous solution using degreased coffee bean. *J. Hazard. Mater.* **176**, 820–828.

Bingöl, D., Veli, S., Zor, S. & Özdemir, U. 2012 Analysis of adsorption of reactive azo dye onto $CuCl_2$ doped polyaniline using Box–Behnken design approach. *Synthetic Metal.* **162**, 1566–1571.

Chowdhury, S., Mishra, R., Saha, P. & Kushwaha, P. 2011 Adsorption thermodynamics, kinetics and isosteric heat of adsorption of malachite green onto chemically modified rice husk. *Desalination* **265**, 159–168.

Das, D., Vimala, R. & Das, N. 2014 Biosorption of Zn(II) onto Pleurotus platypus: 5-Level Box–Behnken design, equilibrium, kinetic and regeneration studies. *Ecol. Eng.* **64**, 136–141.

Ding, F., Li, X.-N., Diao, J.-X., Sun, Y., Zhang, L., Ma, L., Yang, X.-L., Zhang, L. & Sun, Y. 2012 Potential toxicity and affinity of triphenylmethane dye malachite green to lysozyme. *Ecotoxicol. Environ. Safety* **78**, 41–49.

Du, L.-N., Zhao, M., Li, G., Xu, F.-C., Chen, W.-H. & Zhao, Y.-H. 2013 Biodegradation of malachite green by *Micrococcus* sp. strain BD15: biodegradation pathway and enzyme analysis. *Int. Biodeterior. Biodegrad.* **78**, 108–116.

Gong, R., Feng, M., Zhao, J., Cai, W. & Liu, L. 2009 Functionalization of sawdust with monosodium glutamate for enhancing its malachite green removal capacity. *Bioresour. Technol.* **100**, 975–978.

Hameed, B. & El-Khaiary, M. 2008 Malachite green adsorption by rattan sawdust: isotherm, kinetic and mechanism modeling. *J. Hazard. Mater.* **159**, 574–579.

Jain, M., Garg, V. & Kadirvelu, K. 2011 Investigation of Cr VI adsorption onto chemically treated *Helianthus annuus*: optimization using response surface methodology. *Bioresour. Technol.* **102**, 600–605.

Khattri, S. & Singh, M. 2009 Removal of malachite green from dye wastewater using neem sawdust by adsorption. *J. Hazard. Mater.* **167**, 1089–1094.

Kumar, A., Kumar, Sh. & Kumar, S. 2003 Adsorption of resorcinol and catechol on granular activated carbon: equilibrium and kinetics. *Carbon* **41**, 3015–3025.

Kumar, K. V., Sivanesan, S. & Ramamurthi, V. 2005 Adsorption of malachite green *Pithophora* sp., a fresh water algae: equilibrium and kinetic modelling. *Process Biochem.* **40**, 2865–2872.

Michaux, F., Carteret, C., Stébé, M.-J. & Blin, J.-L. 2013 Investigation of properties of mesoporous silica materials based on nonionic fluorinated surfactant using Box–Behnken experimental designs. *Micropor. Mesopor. Mater.* **174**, 135–143.

Mittal, A., Thakur, V., Mittal, J. & Vardhan, H. 2014 Process development for the removal of hazardous anionic azo dye Congo red from wastewater by using hen feather as potential adsorbent. *Desalin. Water Treat.* **52**, 227–237.

Mourabet, M., El Rhilassi, A., El Boujaady, H., Bennani-Ziatni, M., El Hamri, R. & Taitai, A. 2012 Removal of fluoride from aqueous solution by adsorption on Apatitic tricalcium phosphate using Box–Behnken design and desirability function. *Appl. Surf. Sci.* **258**, 4402–4410.

Podstawczyk, D., Witek-Krowiak, A., Chojnacka, K. & Sadowski, Z. 2014 Biosorption of malachite green by eggshells: mechanism identification and process optimization. *Bioresour. Technol.* **160**, 161–165.

Roosta, M., Ghaedi, M., Shokri, N., Daneshfar, A., Sahraei, R. & Asghari, A. 2014 Optimization of the combined ultrasonic assisted/adsorption method for the removal of malachite green by gold nanoparticles loaded on activated carbon: experimental design. *Spectrochim. Acta A* **118**, 55–65.

Shahbazi, A., Younesi, H. & Badiei, A. 2014 Functionalized nanostructured silica by tetradentate-amine chelating ligand as efficient heavy metals adsorbent: applications to industrial effluent treatment. *Korean J. Chem. Eng.* **31**, 1598–1607.

Shedbalkar, U. & Jadhav, J. 2011 Detoxification of malachite green and textile industrial effluent by Penicillium ochrochloron. *Biotechnol. Bioproc. E* **16**, 196–204.

Srivastava, S., Sinha, R. & Roy, D. 2004 Toxicological effects of malachite green. *Aquatic Toxicol.* **66**, 319–329.

Wan Ngah, W. S. & Hanafiah, M. A. K. M. 2008 Removal of heavy metal ions from wastewater by chemically modified plant wastes as adsorbents: a review. *Bioresour. Technol.* **99**, 3935–3948.

Wang, H., Yuan, X., Zeng, G., Leng, L., Peng, X., Liao, K., Peng, L. & Xiao, Z. 2014 Removal of malachite green dye from wastewater by different organic acid-modified natural adsorbent: kinetics, equilibriums, mechanisms, practical application, and disposal of dye-loaded adsorbent. *Environ. Sci. Pollut. Res. Int.* **21**, 11552–11564.

Witek-Krowiak, A. 2011 Analysis of influence of process conditions on kinetics of malachite green biosorption onto beech sawdust. *Chem. Eng. J.* **171**, 976–985.

First received 28 September 2014; accepted in revised form 9 December 2014. Available online 24 January 2015